02

XPS and NEXAFS studies of bismuth tantalate with pyrochlore structure doped with Cu/Co

© K.N. Parshukova[1*], S.V. Nekipelov[2], A.V. Koroleva[3], A.M. Lebedev[4], B.A. Makeev[5], R.I. Korolev[1], N.A. Zhuk[1]

[1*] Syktyvkar State University, Syktyvkar, Russia
[2] Institute of Physics and Mathematics of the Komi Scientific Center of the Ural Branch of the Russian Academy of Sciences, Syktyvkar, Russia
[3] National Research Center „Kurchatov Institute“, Moscow, Russia
[5] Institute of Geology of the Komi Scientific Center of the Ural Branch of the Russian Academy of Sciences, Syktyvkar, Russia

e-mail: kristinaparshukova17@gmail.ru

Received May 03, 2025
Revised June 12, 2025
Accepted October 24, 2025

The chemical state of metal cations in the pyrochlore $Bi_2Cu_{1/2}Co_{1/2}Ta_2O_{9\pm\delta}$ (space group $Fd-3m$, $a = 10.5379(8)$ Å) was characterized using XPS and NEXAFS spectroscopy. ased on the shift of the XPS Ta4f spectrum toward lower energies by 0.9 eV, the effective charge of tantalum cations $+(5-\delta)$ was determined. The NEXAFS Cu2p spectra of the pyrochlore represent a superposition of spectra from Cu(I) and Cu(II) cations. According to the analysis of relative peak intensities in the XPS Cu2p spectrum, the Cu(I)/Cu(II) ratio is 9/11. The nature of the NEXAFS and XPS Co2p spectra indicates the charge state Co(II,III).

Keywords: pyrochlore, NEXAFS, XPS, 3d-elements, charge state of ions.

DOI: 10.61011/EOS.2025.10.62551.7972-25

Introduction

Unwavering interest in oxide pyrochlores stems from their wide range of practically useful properties. They are known as photocatalysts, dielectrics, ionic and metallic conductors, and exhibit ferri- and ferrimagnetism, giant magnetoresistance, superconductivity, and spin glass states [1–3]. The crystal structure of oxide pyrochlores $A_2B_2O_6O'$ is stable against cationic substitutions in both sublattices A_2O' and B_2O_6 as well as against oxygen vacancies in the A_2O' sublattice, allowing wide variation in the chemical composition of complex oxides. Traditionally, octahedral B sites are occupied by relatively small and electronegative tetravalent and pentavalent cations (Ti^{4+}, Nb^{5+}, Ta^{5+}), while larger divalent or trivalent ions (Bi^{3+}, Ca^{2+}) are distributed in eight-coordinated A sites [4]. Bismuth-containing pyrochlores attract particular attention. Synthetic bismuth-containing pyrochlores are promising for multilayer ceramic capacitors and microwave dielectric components due to low dielectric losses, high dielectric permittivity, and chemical compatibility with low-melting copper conductors. Bismuth tantalate$BiTaO_4$ does not crystallize in the pyrochlore structure. The pyrochlore structure is stabilized by doping bismuth orthotantalate 3d-ions [5,6], resulting in a partially vacant bismuth sublattice and distribution of the dopant impurity across both bismuth and tantalum cationic sublattices, inducing relaxation processes in the ceramics [7]. The mixed distribution of 3d-ions across the two cationic pyrochlore sublattices arises due to the limited capacity of the octahedral sublattice for 3d-cations. Recent studies have shown that multi-element pyrochlores can be successfully synthesized, with various transition element cations in the octahedral sublattice [8,9]. Studies of multicomponent pyrochlores are scarce. At present, the mutual influence of transition elements on ceramic properties remains insufficiently explored. As shown in [8,9], the complex pyrochlore $Bi_{2-1/3}Cr_{1/6}Mn_{1/6}Fe_{1/6}Co_{1/6}Ni_{1/6}Cu_{1/6}Zn_{1/6}Ta_2O_{9+\Delta}$ exhibits averaged dielectric parameters compared to singly doped pyrochlores. It has been suggested that the individual effects of transition element ions in multi-element pyrochlores are offset by the combined influence of all dopants. The phase formation process during solid-state synthesis was studied in detail in [8].

The present work demonstrates the possibility of synthesizing single-phase pyrochlore $Bi_2Cu_{1/2}Co_{1/2}Ta_2O_{9\pm\delta}$and analyzes the charge states of transition element ions based on X-ray spectroscopy data (NEXAFS, XPS).

Experimental part

Synthesis of pyrochlore $Bi_2Cu_{1/2}Co_{1/2}Ta_2O_{9\pm\delta}$ was performed by solid-state reaction from a stoichiometric mixture of Bi(III), Cu(II), Ta(V), and Co(II,III) oxides via stepwise calcination at 650, 850, 950, and 1050 °C. The finely ground oxide mixture was preliminarily compacted into disks and calcined in air in corundum crucibles for 15 h at each stage. After each calcination stage, the samples were thoroughly ground in an agate mortar and re-pressed using a manual acrylic press. X-ray phase analysis (XPA) was conducted

using a Shimadzu 6000 diffractometer (Cu K_α radiation, $2\theta = 10^\circ - 70^\circ$, scan speed 2.0°/min). Surface morphology and quantitative chemical analysis of the samples were performed using a Tescan VEGA 3LMN scanning electron microscope and INCA Energy 450 energy-dispersive spectrometer. NEXAFS was conducted at the NanoPES station of the KISI synchrotron source at the Kurchatov Institute. NEXAFS spectra were obtained by total electron yield detection with energy resolutions of 0.5 and 0.7 eV in the Cu2p and Co2p absorption edge regions, respectively. XPS analysis was performed on a Thermo Scientific ESCALAB 250Xi spectrometer Al K_α radiation, 1486.6 eV) with an ion-electron charge compensation system. All peaks were calibrated relative to the C1s peak at 284.6 eV. Data processing utilized the ESCALAB 250 Xi spectrometer software.

Energy positions of XPS spectrum components for $Bi_2Cu_{1/2}Co_{1/2}Ta_2O_{9\pm\delta}$

Peak	Energy, eV	Peak	Energy, eV	Peak	Energy, eV
Bi4$f_{7/2}$	158.9	Co2$p_{3/2}$	780.8	Cu(I)2$p_{1/2}$	951.1
Bi4$f_{5/2}$	164.2	Co2$p_{1/2}$	796.6	Cu(II)2$p_{1/2}$	953.3
Bi5$d_{5/2}$	26.0	Co sat	786.0	Cu2p sat	961.3
Bi5$d_{3/2}$	29.0	Co sat	801.8	Co sat	801.8
Ta4$f_{7/2}$	25.6	Cu(I)2$p_{3/2}$	931.5	Cu(I)2$p_{3/2}$	931.5
Ta4$f_{5/2}$	27.4	Cu(II)2$p_{3/2}$	933.6	Cu(II)2$p_{3/2}$	933.6
Ta5$p_{3/2}$	35.8	Cu2p sat	941.8		

Results and Discussion

According to XPA data, the $Bi_2Cu_{1/2}Co_{1/2}Ta_2O_{9\pm\delta}$ sample is single-phase and crystallizes in the cubic pyrochlore structural type (space group $Fd-3m$). The lattice cell parameter of $Bi_2Cu_{1/2}Co_{1/2}Ta_2O_{9\pm\delta}$ is 10.5379(8) Å and differs little from the lattice cell constant of 10.54051(3) Å for the cobalt-containing pyrochlore $Bi_{1.86}CoTa_2O_{9\pm\delta}$ [10]. The similar lattice cell parameter values arise from the close radii of Cu(II) and Co(II) cations (R (Cu(II), CN = 6) = 0.73 Å, R (Co(II), CN = 6) = 0.745 Å), despite the deviation from the stoichiometric coefficient at bismuth. The reduced lattice cell parameter of the studied pyrochlore is associated with the distribution of some transition element cations at the bismuth site, as noted previously in [10]. As shown below, the pyrochlore $Bi_2Cu_{1/2}Co_{1/2}Ta_2O_{9\pm\delta}$ contains Cu(I) cations, whose radius is substantially larger than that of Cu(II) (R (Cu(I), CN = 6) = 0.77 Å) making the distribution of Cu(I) cations at the Bi(III) site highly probable. Elemental mapping of the $Bi_2Cu_{1/2}Co_{1/2}Ta_2O_{9\pm\delta}$ sample revealed uniform distribution of all element atoms across the surface, and EDS analysis confirmed agreement between the experimental and nominal sample compositions. According to the EDS spectrum, the chemical composition of the sample corresponds to the formula $Bi_{1.94}Co_{0.49}Cu_{0.38}Ta_2O_{9\pm\delta}$ and is close to the nominal composition. The reduced stoichiometric coefficient for copper atoms in the pyrochlore formula is due to an error in determining the relative intensity of the copper absorption line caused by overlap of copper K-series and tantalum L-series lines in the 8 eV region. The pyrochlore $Bi_2Cu_{1/2}Co_{1/2}Ta_2O_{9\pm\delta}$ exhibits a low-porosity, grainless, dense microstructure. The average crystallite size, determined by X-ray diffraction using the Scherrer formula, is 64 nm. The grainless ceramic microstructure results from the interaction of low-melting precursors — Cu(II), Co(II), and Bi(III) oxides. Fig. *a* shows XPS spectra of the pyrochlore over a wide energy range, as well as spectral dependencies in the ionization threshold regions for Bi4f, Bi5d, Ta4f, Co2p and Cu2p of the studied sample (Fig. *b, d, f, h*). The figures present the results of decomposing spectral dependencies into individual peaks modeled by Gauss-–Lorentz curves. Analysis of the panoramic spectrum revealed the C1s peak (Fig. *a*), associated with surface organic contamination of the sample. The presence of contaminants introduces an indeterminate contribution to the O1$s$peak intensity; therefore, metal spectra were used for surface chemical composition analysis. The XPS Bi4f spectra of the sample and Bi_2O_3 oxide (Fig. *b*) match in composition and energy positions of spectral features, with no splitting or distortion of peaks observed. This indicates that all bismuth cations in the pyrochlore are in the same charge state +3. In the tantalum cation spectra, a characteristic shift toward lower energies is observed compared to the binding energy in the pentavalent tantalum oxide Ta_2O_5, which occurs when the effective positive charge decreases. Specifically, for the spectra Ta4f and Ta5p presented here, the energy shift for $Bi_2Cu_{1/2}Co_{1/2}Ta_2O_{9\pm\delta}$ amounts to 0.9 eV (Fig. *c*). This indicates that tantalum cations have a lower effective charge $+(5-\delta)$, presumably because low-charge transition element cations are predominantly distributed in the octahedral positions of Ta(V), thereby indirectly reducing its effective charge.

The energy range of the Co2p spectrum includes the peak (Fig. *d*) corresponding to the binding energy of the Bi4$p_{1/2}$level. Meanwhile, comparing the pyrochlore spectrum with our spectra of Co_3O_4 and the literature data for CoO [11], it can be noted that the energy positions of the main peaks in the pyrochlore spectrum nearly coincide with those of CoO. In both spectra, satellite peaks at 786 and 802 eV are clearly pronounced, characteristic of double-charged Co(II) cations (table). At the same time, the energy position of the Co2$p_{3/2}$ peak in the pyrochlore is shifted toward higher energies compared to the CoO spectrum. In this case, it can be assumed that cobalt cations in the pyrochlore are in a mixed valence state Co(II,III). A similar conclusion regarding the charge state of cobalt cations in $Bi_2Cu_{1/2}Co_{1/2}Ta_2O_{9\pm\delta}$ can be drawn from

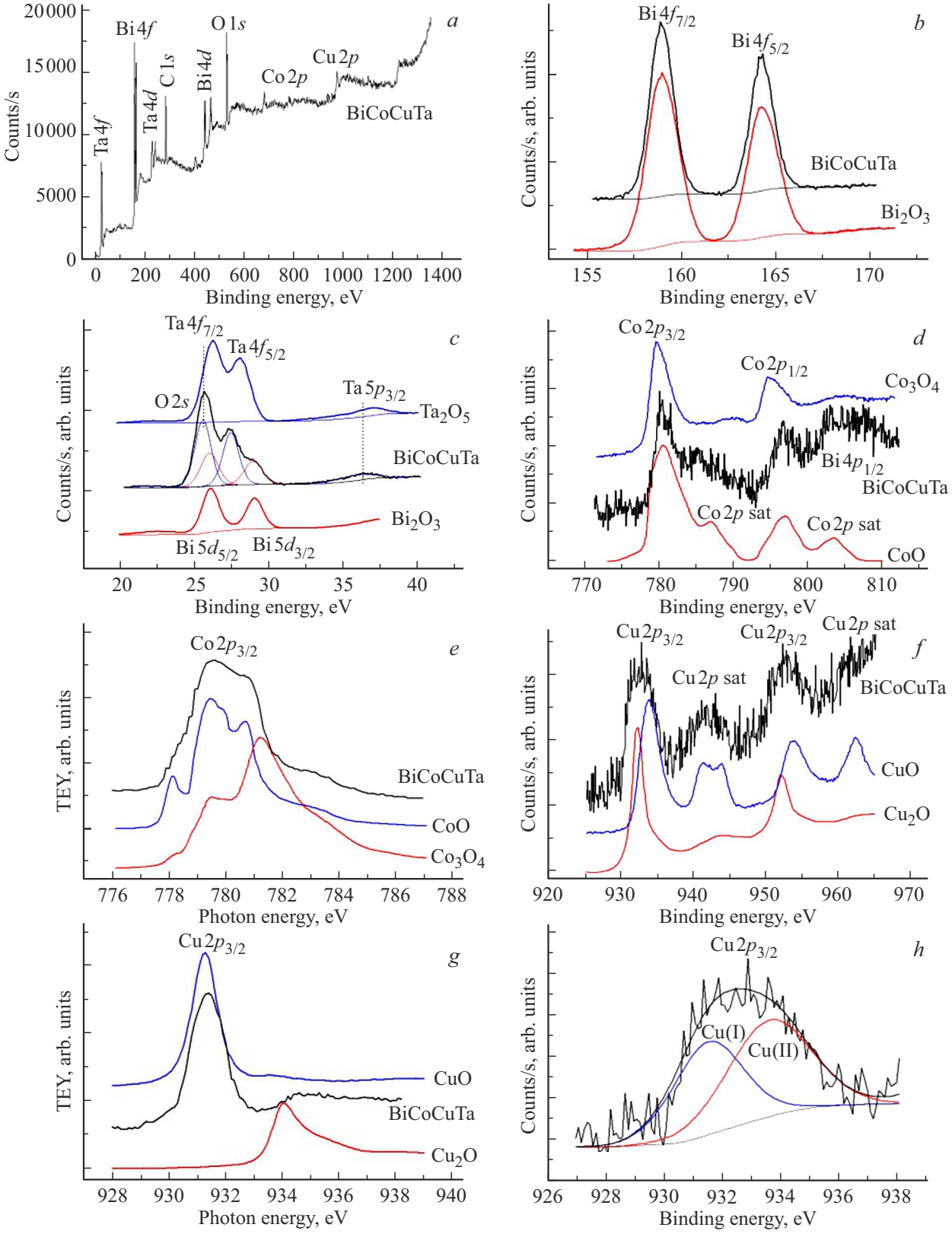

Survey XPS spectrum (*a*), XPS Bi4*f* (*b*) and Ta4*f* (*c*), Co2*p* (*d*) and Cu2*p* (*e*), NEXAFS Co2*p* (*f*) and Cu2*p* (*g*) spectra of oxides and $Bi_2Cu_{1/2}Co_{1/2}Ta_2O_{9\pm\delta}$ (BiCuCoTa), decomposition of the XPS Cu2$p_{3/2}$ BiCuCoTa spectrum of BiCuCoTa into Cu(I) and Cu(II) *h*.)

the analysis of NEXAFS Co2p spectra of the pyrochlore and cobalt oxides, shown in Fig. *e*. From Fig. *e*, it is evident that the absorption spectrum of the pyrochlore in the Co2p absorption edge region represents a superposition of CoO [12] and Co_3O_4 spectra. This is indicated by the broad-band nature of the$Co2p_{3/2}$ spectrum of the pyrochlore, the absence of splitting in the 778 eV region, and the comparable intensity ratio of spectral components at 779.5 and 781 eV, resulting from the superposition of the absorption band from Co(III) cations. Comparing the XPS Cu2p spectrum of the pyrochlores with the spectra of CuO and Cu_2O [13,14] it can be noted (Fig. *f*) that the energy positions of the main peaks in the complex pyrochlore spectrum (934 and 953 eV) nearly coincide with those of CuO. Additionally, both the pyrochlore and CuO oxide spectra exhibit satellite peaks. Notably, the pyrochlore spectra show shoulders in the 931.5 and 951 eV regions, characteristic of Cu_2O. is provides grounds to conclude that copper ions in the pyrochlore composition have two nonequivalent charge states: Cu(I) and Cu(II). A similar conclusion regarding the charge state of copper atoms can be drawn from the analysis of NEXAFSCu2p spectra of the pyrochlore and copper oxides, presented in Fig. 1, *g*.

Fig. 1, *g* clearly shows that the copper spectrum in the pyrochlore, besides the Cu(II) signal at 931.5 eV, contains a signal characteristic of Cu(I) at 934 eV. To determine the contributions of different valence states of copper, we decomposed the XPS $Cu2p_{3/2}$ spectrum into individual peaks from Cu(I) and Cu(II) cations, modeled by Gauss–Lorentz curves. The modeling results for the $Cu2p_{3/2}$ level in $Bi_2Cu_{1/2}Co_{1/2}Ta_2O_{9\pm\delta}$are presented in Fig. 1, *h*. From the modeled spectrum, it is evident that copper cations are present in the monovalent Cu(I) and bivalent Cu(II) states. The proportion of copper cations in each charge state was qualitatively assessed from the ratio of the areas of the corresponding peaks S(Cu(I))/S(Cu(II)) The obtained value for $Bi_2Cu_{1/2}Co_{1/2}Ta_2O_{9\pm\delta}$ is 0.82, i.e., for every 4 atoms in the Cu+ charge state, there are 5 atoms in the Cu^{2+} charge state. The amount of Cu(I) cations in the pyrochlore $Bi_2Co_{1/2}(Cu^{+}_{9/40}Cu^{2+}_{11/40})Ta_2O_{9\pm\delta}$ constitutes approximately 45% of the total copper cations. The presence of Cu(I) ions in a single-phase copper-doped pyrochlore is a nontrivial result, detected using NEXAFS spectroscopy. It can be assumed that in pyrochlores doped with cations in variable oxidation states, electron exchange is possible, enabling electron transfer from Co(II) ions to Cu(II) cations. The need to reduce some copper cations is likely dictated by the system's tendency to stabilize the pyrochlore crystal structure by relieving strains caused by heterovalent doping. Cu(II) cations cause charge imbalance in the Ta(V) sublattice and, being Jahn-Teller cations, induce distortions of the coordination polyhedron. Meanwhile, the reduction of some Cu(II) cations to Cu(I) promotes the oxidation of an equivalent portion of cobalt cations to the Co(III) state, which, due to their small radius and high charge, do not leave the octahedral sublattice. Thus, the more Cu(I) cations present, the more Co(III) cations in the octahedral sublattice. Since the ionic radius of Cu(I) is substantially larger than that of Ta(V) cations (R (Ta(V), acid index = 6) = 0.64 Å), (R (Cu(I), CN = 6) = 0.77 Å), it can be assumed that Cu(I) ions are predominantly distributed in the Bi(III) cation sublattice. Thus, copper-containing pyrochlores based on bismuth tantalate contain Cu(I) cations, the reasons for their formation remaining insufficiently clear. If electron exchange between dopant ions in transitional oxidation states is possible, this opens prospects for controlling the valence states of transition elements by varying the qualitative composition of dopants, and consequently, their distribution across cation sublattices and regulation of relaxation processes in ceramics.

Conclusions

The pyrochlore $Bi_2Cu_{1/2}Co_{1/2}Ta_2O_{9\pm\delta}$as investigated using X-ray spectroscopy methods. The XPS Ta4f spectrum exhibits a characteristic shift toward lower energies by 0.9 eV, associated with the distribution of low-charge transition element cations in the octahedral positions of Ta(V). The effective charge of tantalum cations is $+(5-\delta)$. Cobalt cations in the pyrochlore predominantly have the charge +2, +3. The NEXAFS Cu 2p spectra of the oxide ceramics represent a superposition of absorption bands from Cu(I) and Cu(II) cations. The molar ratio of Cu(I)/Cu(II) cations in the pyrochlore is 0.82.

Acknowledgments

XPS studies were performed using the equipment of the Resource Center „Physical Methods of Surface Investigation“ at the Scientific Park of St. Petersburg State University. NEXAFS studies were conducted using synchrotron radiation from the storage ring of the „NanoPES“ station (NRC „Kurchatov Institute“).

Conflict of interest

The authors declare that they have no conflict of interest.

References

[1] G. Giampaoli, T. Siritanon, B. Day, J. Li, M.A. Subramanian. Prog. Sol. St. Chem., **50**, 16–23 (2018). DOI: 10.1016/j.progsolidstchem.2018.06.001
[2] Z. Hiroi, J.-I. Yamaura, S. Yonezawa, H. Harima. Physica C, **460–462** (1), 20–27 (2007). DOI: 1016/j.physc.2007.03.023
[3] J.E. Greedan. J. All. Comp., **408–412**, 444–455 (2006). DOI: 10.1016/j.jallcom.2004.12.084
[4] M.A. Subramanian, G. Aravamudan, G.V. Subba Rao. Prog. Sol. St. Chem., **15**, 55–143 (1983). DOI: 10.1016/0079-6786(83)90001-8
[5] M.W. Lufaso, T.A. Vanderah, I.M. Pazos, I. Levin, R.S. Roth, J.C. Nino, V. Provenzano, P.K. Schenck. J. Sol. St. Chem., **179**, 3900–3910 (2006). DOI: 10.1016/j.jssc.2006.08.036

[6] G.C. Miles, A.R. West. J. Am. Ceram. Soc., **89**, 1042–1046 (2006). DOI: 10.1111/j.1551-2916.2005.00799.x
[7] M. Valant. J. Am. Ceram. Soc., **92** (4), 955–958 (2009). DOI: 10.1111/j.1551-2916.2009.02984.x
[8] E.P. Rylchenko, B.A. Makeev, D.V. Sivkov, R.I. Korolev, N.A. Zhuk. Lett. Mater., **12** (4s), 486–492 (2022). DOI: 10.22226/2410-3535-2022-4-486-492
[9] K.N. Parshukova, E.P. Rylchenko, V.A. Muravyev, K.A. Badanina, B.A. Makeev, R.I. Korolev, N.A. Zhuk. Glass and ceramics, **5**, 34–39 (2022). DOI: 10.1007/s10717-023-00523-70
[10] N.A. Zhuk, M.G. Krzhizhanovskaya, N.A. Sekushin, D.V. Sivkov, I.E. Abdurakhmanov. J. Mater. Res. Technol., **22**, 1791–1799 (2023). DOI: 10.1016/j.jmrt.2022.12.059
[11] M. Hassel, H.-J. Freund. Surf. Sci. Spectra, **4**, 273–278 (1996). DOI: 10.1116/1.1247797
[12] T.J. Regan, H. Ohldag, C. Stamm, F. Nolting, J. Luning, J. Stöhr. Phys. Rev. B, **64** (21), 214422 (2001). DOI: 10.1103/PhysRevB.64.214422
[13] D. Barreca, A. Gasparotto, E. Tondello. Surf. Sci. Spectra, **14**, 41–51 (2007). DOI: 10.1116/11.20080701
[14] M. Grioni, J.F. van Acker, M.T. Czyžyk, J.C. Fuggle. Phys. Rev B, **45**, 3309–3318 (1992). DOI: 10.1103/PhysRevB.45.3309

Translated by J.Savelyeva